Bol. Soc. Paran. Mat.
©SPM – E-ISSN-2175-1188
SPM: www.spm.uem.br/bspm

(3s.) **v. 2026 (44) 7** : 1–20.
ISSN-0037-8712
doi:10.5269/bspm.81798

Computational Study of Mixed Convection Magnetohydrodynamics Flow of an Engine Oil Hybrid Nanofluid Over a Stretchable Cylinder in a Porous Environment with Heat Source/Sink Effects

Poornima Samaje, Salma Allabaksh, Sibyala Vijayakumar Varma and Hanumagowda Bannihalli Naganagowda

ABSTRACT: This work presents the steady magnetohydrodynamic (MHD) boundary-layer flow and heat transmission of an Al_2O_3-MWCNT/engine-oil hybrid nanofluid along a stretching cylindrical surface within a Darcy porous medium, influenced by internal heat generation or absorption. The thermophysical properties of hybrid nanoparticles, including altered effective density, viscosity, heat capacity, and thermal conductivity, are incorporated into the conventional nanofluid formulation. The governing partial differential equations are simplified using similarity transformations into a coupled system of nonlinear ordinary differential equations, which are subsequently solved numerically using the MATLAB bvp4c method. The velocity, temperature, skin-friction coefficient, and Nusselt number are analyzed with respect to the magnetic parameter, porosity, curvature, volume fraction of the nanoparticle, Prandtl number, and heat source/sink. The results demonstrate that although the viscosity increase slightly diminishes momentum, heat transmission is significantly improved by hybrid nanofluid formulations compared to single-nanoparticle suspensions. The enhanced thermal performance derived from the synergistic effects of Al_2O_3 and MWCNT nanoparticles indicates that hybrid nanofluids are effective in increasing heat transfer in surface stretching engineering processes.

Key Words: MHD, stretching cylinder, boundary layer, heat source/sink, heat transfer.

Contents

1. Introduction

A variety of industrial and engineering processes, such as polymer extrusion, fiber coating, lubrication systems, and thermal management of rotating gear, include stretching cylinder flows. Mukhopadhyay [1] investigated the influence of permeability and curvature on mixed convection boundary layer flow over a stretching cylinder embedded in a porous medium. Due to its exceptional lubricating properties and thermal stability, engine oil is commonly employed in mechanical and automotive systems. Nonetheless, heat dissipation is constrained by its minimal thermal conductivity. A proficient method for enhancing heat transfer efficacy is the incorporation of nanoparticles, particularly hybrid nanofluids ([2]- [3]). The investigation of mixed-convection boundary-layer flow across stretched geometries has garnered significant attention recently, owing to its vital role in polymer extrusion, wire drawing, lubrication processes, and thermal management systems in porous and geophysical contexts ([4]- [6]). In example, the stretching cylinder configuration provides a more precise representation of thin filaments, fiber coatings, and

2020 *Mathematics Subject Classification:* 05C50,05C90.
Submitted February 07, 2026. Published April 11, 2026

petroleum wellbore structures than the conventional stretching-sheet model, especially when curvature effects approximate the boundary layer thickness. Previous studies on the stretching of cylinders in porous media primarily focused on Newtonian fluids under forced or mixed convection, permeability resistance, and thermal boundary-layer properties; they did not consider advanced mechanisms for enhancing energy transport such as internal heat generation, magnetic-field influence, or nanofluid thermodynamics ([7]- [9]). Hybrid nanofluids, created by suspending two different nanoparticles in a standard base fluid, have emerged as effective engineering coolants due to their synergistic capacity to enhance heat transfer, stabilize suspension properties, and augment thermal conductivity, addressing the increasing demand for high-performance cooling and lubricating fluids. The hybrid combination of aluminum oxide Al_2O_3 and multi-walled carbon nanotubes (MWCNTs) suspended in engine oil has garnered significant interest due to MWCNTs' exceptional axial heat conduction and micro-scale thermal dispersion, while Al_2O_3 improves thermophysical stability ([10]- [11]). Engine oil-based hybrid nanofluids are essential due to their role in enhancing heat dissipation and controlling shear loading in tribological systems, rotating shafts, petroleum drilling components, and porous-medium heat exchangers. Saeed et al. [12] studied the heat and mass transport of carbon nanotubes and Fe_3O_4 hybrid nanofluid flow over a stretching curved surface influenced by Darcy-Forchheimer effects. The heat transfer rate rose by 2.21%, 2.1%, and 2.3% for MWCNTs, SWCNTs, and Fe_3O_4 nanoparticles, respectively.

One area of physics called magnetohydrodynamics (MHD) examines the reciprocal magnetic interaction and electrical energy transfer to moving fluids. The hydro magnetic phenomenon is becoming more significant due to its numerous applications in engineering and industry, including MHD throttles, automotive fuel level indicators, accelerators, nuclear reactors, electroslag remelting, alloy refinement, magnetometers, electronic motors, and transformers. Manjunath et al. [13] investigated how varied viscosity affected the MHD hybrid nanofluid flow's boundary layer thickness and came to the conclusion that both variable viscosity and the volume fraction of nano-granules improved heat transfer in the flow field. Furthermore, in electrically conducting lubricants and petroleum fluids, the application of an external magnetic field creates a magnetohydrodynamic (MHD) Lorentz force that alters momentum transport and creates an additional damping mechanism that can be used to control flow stability and boundary-layer development ([14]- [15]). In both endothermic and exothermic reaction settings, dissipation-dominated flows, and porous thermal processing systems, the existence of internal heat generation or absorption (heat source/sink) is crucial. Comprehensive studies integrating MHD, heat source/sink mechanisms, and hybrid-nanofluid transport over a stretching cylinder embedded in a porous medium under mixed-convection conditions are still largely unexplored, despite the fact that several studies have examined MHD effects, porous resistance, or nanofluid heat transfer separately. Nath et al. [16] investigated the effects of thermal stratification on the magnetohydrodynamics (MHD) flow of ternary hybrid nanofluids, specifically $Cu - Al_2O_3 - TiO_2$ suspended in water, past a vertically stretching cylinder in a porous medium and concludes that thermal stratification reduces the velocity and temperature of the ternary hybrid nanofluid compared to scenarios without stratification, while also demonstrating superior heat transfer rates compared to hybrid and ordinary nanofluids. Ismail et al. [17] studied the effects of thermal radiation on MHD hybrid nanofluid flow and Mathematical model transformed into ODE's, solved numerically using MATLAB. Hayat et al. [18] investigated the enhancement of heat transfer in nanofluid flow under the influence of an inclined magnetic field, nonlinear radiation, and heat source/sink, noting that increased values of nonlinear thermal radiation and heat generation/absorption parameters augmented the thickness of the temperature boundary layer. Ali et al. [19] investigated the phenomenon of a constant hydromagnetic flow of an incompressible electrically conducting fluid over an inclined stretching sheet, induced by a linearly stretching surface. The researchers discovered that the thickness of the temperature boundary layer in fluid flow was considerably affected by the magnetic factor, angle of inclination, Prandtl number, and Eckert number. Gururaj ([20]- [21]) examined the hydromagnetic flow over nonlinear stretching surfaces affected by radiation and a fluctuating magnetic field. The skin friction coefficient and velocity boundary layer thickness were dramatically affected by the intensity of the changing magnetic field. Moreover, an extensive body of research investigates both steady and unsteady magnetohydrodynamic (MHD) flow across diverse physical conditions and applications ([22]- [26]). Thermal radiation is the process by which heat energy is emitted from a radiated surface in all directions as electromagnetic waves. Radiative heat transfer is the sole method of heat transfer in a

vacuum. This process substantially influences the development of high temperatures. In engineering and science, thermal radiation significantly influences heat transfer and the movement of various liquids. Moreover, space technology, which seeks to attain maximal thermal efficiency for apparatus functioning at exceedingly high temperatures, significantly depends on the phenomena of heat radiation. Khan et al. [27] analyzed the nonlinear Sisko fluid flow past an expanding cylinder with a stagnation point, revealing that the Prandtl number significantly affects the temperature profile's decline and the thermal boundary layer's thickness. Hayat et al. [28] investigated the influence of magnetic fields and nonlinear thermal radiation on the boundary layer flow of viscous fluid over an extending cylinder, revealing that the magnetic number, Rosseland thermal factors, and Prandtl number significantly govern shear stresses and heat transfer. Hayat et al. [29] investigated the nonlinear thermal mixed convection problem including Maxwell nanofluid flow over an expanding cylinder affected by a chemical reaction. They indicated that physical parameters, including the Biot number, chemical reactions, and Brownian motion, significantly improved the heat and mass transfer in the flow of Maxwell nanofluid. This emerging category of nanofluids, known as hybrid nanofluids, possesses extensive potential applications across several domains of heat transfer, encompassing microelectronics, microfluidics, transportation, manufacturing, medicine, defence, acoustics, naval construction, and propulsion. Besides their exceptionally high effective thermal conductivity, hybrid nanofluids can offer significant advantages when nanoparticles are adequately disseminated. For example, nanofluid flow is recognized for its superior heat transfer capabilities compared to conventional fluids. Choi et al. [30] were the first to propose that the integration of nanoparticles into the fluid can improve heat transfer. Hussein et al. [31] discovered that the maximum Nusselt number ratio for the 3% hybrid nanofluid was 50% higher than the results for EG flows in their study on the impact of AlN hybrid nanoparticles on heat transfer and pressure decrease in a horizontal circular tube. Hamid et al. [32] examined thermal conductivity as one of the features of hybrid nanofluids. It was shown that at a concentration of 3.0% and a temperature of $70C$, the thermal conductivity of the hybrid nanofluid rose by as much as 22.1%. Boukerma [33] investigated the impact of EG-water mixtures, with mass percentages from 0% to 100% ethylene glycol, on the Reynolds number, volume fractions, and the flow and convective heat transfer characteristics of various nanoparticles. The extraction of a plastic panel, the coolant for a metallic panel submerged in a cooling bath, the incessant dyeing and rotation of threads, the dyeing of synthetic fibers, the boundary layer of liquid films during the condensation process, among others, exemplify the myriad practical applications of heat transfer issues in the boundary layer for an extending sheet or cylinder in engineering processes. In alignment with the applications, Wang [34] was the pioneer in examining the flow around a stretching cylinder and found that third-order ordinary differential equations may effectively resolve the Navier-Stokes equation. To enhance the heat removal rate, Maskeen et al. [35] investigated the influence of Lorentz force and thermal radiation on the flow of an alumina copper/water $Al_2O_3 - Cu/H_2O$ hybrid nanofluid over an extended cylinder and analyzed the flow characteristics of nanoparticles. In comparison to the incorporation of hybrid material, they found that the convective heat transfer rate for copper/water nanofluid is diminished. Vanita and Poply [36] examined the constant slip flow of magnetohydrodynamics along a stretching cylinder, considering the influences of heat generation and external velocity. The concentration profile was seen to grow with larger curvature and thermophoresis parameters, whereas it decreased with the radiation parameter. Ismail and Gururaj [37] observed the effects of variable viscosity and radiation in the flow of MHD hybrid nanofluid past an elongated cylinder. They concluded that thermal radiation, associated with an enhancement of conduction effects, is responsible for the elevation of the thermal plots. Furthermore, numerous scientists ([38]- [40]) have investigated the properties of nanoparticles and nanofluids under diverse physical conditions. This study is distinctive as it concurrently integrates internal heat source/sink, hybrid nanofluid transport, and magnetohydrodynamic (MHD) effects to model mixed convection flow across a stretching cylinder situated within a porous medium. An externally applied magnetic field is incorporated to consider Lorentz force effects, facilitating effective modification of the flow and temperature boundary layers, unlike prior studies that focused solely on conventional fluids and buoyancy-driven mechanisms. Incorporating a heat source/sink term enhances the thermal model, enabling the representation of actual energy generation and absorption processes. This study's primary innovation is the analysis of a hybrid nanofluid composed of Al_2O_3 and multi-walled carbon nanotubes (MWCNTs) dispersed in engine oil, which has not before been explored for stretching cylinder configurations in porous media. To ensure reliable adherence to

the physical boundary conditions, the governing nonlinear boundary layer equations are formulated in a self-consistent manner and resolved utilizing the MATLAB *bvp4c* boundary value problem framework. This study not only delineates its distinctive contribution to the literature on advanced thermal transport in porous media but also elucidates the combined effects of magnetohydrodynamics, heat source/sink, and hybrid nanofluid parameters on flow and heat transfer characteristics, providing innovative scientific insights.

2. Physical Model and Solution of the Problem

A vertically elongated cylinder with radius R is embedded in a fluid-saturated porous medium, constituting the physical model. The radial r direction is perpendicular to the cylinder's surface, whereas the axial x direction is aligned with the cylinder's length. As the cylinder undergoes axial elongation, velocity components u and v are generated in the radial and axial directions, respectively. Magnetohydrodynamic effects are generated by the application of a uniform transverse magnetic field B_0 from the right side of the cylinder. Gravitational acceleration exerts a downward force on a hybrid nanofluid Al_2O_3+MWCNTs dispersed in engine oil, leading to mixed convection inside the porous medium.

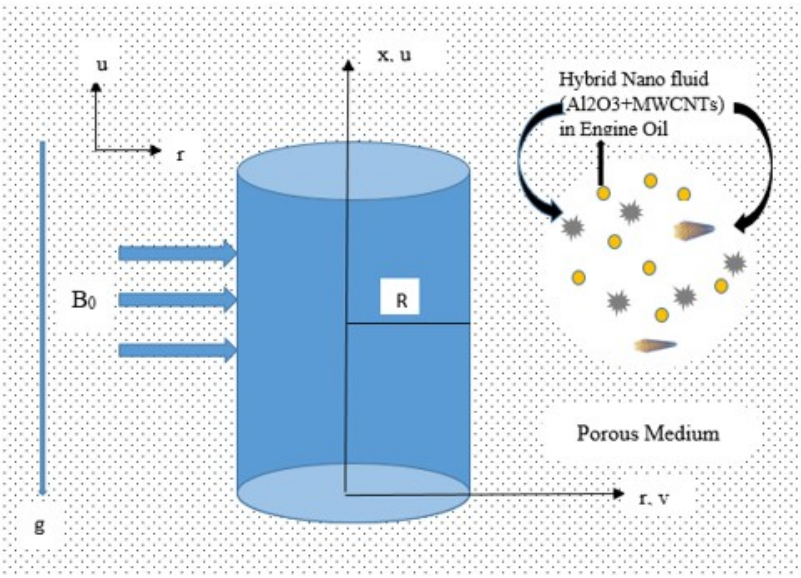

Figure 1: Physical Sketch of the problem.

Governing equations

The governing equations of the present problem are given below:

Continuity Equation:

$$\frac{\partial(ru)}{\partial x} + \frac{\partial(rv)}{\partial r} = 0 \tag{2.1}$$

Momentum Equation:

$$u\frac{\partial u}{\partial x} + v\frac{\partial u}{\partial r} = \nu_{hnf}\left[\frac{1}{r}\frac{\partial}{\partial r}\left(r\frac{\partial u}{\partial r}\right)\right] - \frac{\nu_{hnf}}{K}u - \frac{\sigma_{ehnf}B_0^2}{\rho_{hnf}}u + g\beta_{hnf}(T - T_\infty) \tag{2.2}$$

Energy Equation:

$$u\frac{\partial T}{\partial x} + v\frac{\partial T}{\partial r} = \alpha_{hnf}\left[\frac{1}{r}\frac{\partial}{\partial r}\left(r\frac{\partial T}{\partial r}\right)\right] + \frac{\alpha_{hnf}}{k_{hnf}}Q_0(T - T_\infty) \tag{2.3}$$

Boundary Conditions.
The governing equations are solved under the following boundary conditions:

$$\begin{aligned} &u = U(x), \quad v = 0, \quad T = T_w(x) \quad \text{at} \quad r = R, \\ &u \to 0, \quad T \to T_\infty, \quad \text{as} \quad r \to \infty. \end{aligned} \tag{2.4}$$

Here,

$$U(x) = U_0 \left(\frac{x}{L}\right)$$

is the stretching velocity,

$$T_w(x) = T_\infty + T_0 \left(\frac{x}{L}\right)^N$$

is the prescribed surface temperature (for the forced convection case).

The following similarity variables can be used to simplify Eqs. (2.1)–(2.3) to ODEs:

$$\eta = \frac{r^2 - R^2}{2R}\left(\frac{U}{\nu x}\right)^{1/2}, \quad \psi = (U\nu x)^{1/2} R f(\eta), \quad u = \frac{1}{r}\frac{\partial \psi}{\partial r}, \quad v = -\frac{1}{r}\frac{\partial \psi}{\partial x}, \quad \theta(\eta) = \frac{T - T_\infty}{T_w - T_\infty}. \tag{2.5}$$

When Eq. (2.5) is substituted into Eqs. (2.2)–(2.4), the governing equations become:

$$m_1\left(f'^2 - ff''\right) = m_2\left[2mf'' + (1 + 2\eta m)f'''\right] - m_2 K_1 f' + m_3 \lambda\theta - m_4 M f' = 0 \tag{2.6}$$

$$(Nf'\theta - f\theta') = \frac{m_5}{\mathrm{Pr}}\left(2m\theta' + (1 + 2\eta m)\theta''\right) + \left(\frac{m_5}{m_6}\right)\frac{1}{\mathrm{Pr}}\delta\theta \tag{2.7}$$

$$\begin{aligned} &f' = 1, \quad f = 0, \quad \theta = 1, \text{at} \quad \eta = 0 \\ &f' \to 0, \quad \theta \to 0 \quad \text{as} \quad \eta \to \infty. \end{aligned} \tag{2.8}$$

where

$$m_1 = \frac{\rho_{hnf}}{\rho_f}, \quad m_2 = \frac{\mu_{hnf}}{\mu_f}, \; m_3 = \frac{\beta_{hnf}}{\beta_f}, \quad m_4 = \frac{\sigma_{ehnf}}{\sigma_{ef}}, \; m_5 = \frac{\alpha_{hnf}}{\alpha_f}, \quad m_6 = \frac{k_{hnf}}{k_f}$$

$$M = \frac{\sigma_{e_f} B_0^2}{\rho_f U_0}, \lambda = \frac{g\beta_f T_0 L}{\rho_f U_0^2}, \quad K_1 = \frac{\nu_f L}{U_0 K}, \quad \alpha_{hnf} = \frac{k_{hnf}}{(\rho c_p)_{hnf}}, \quad v_{hnf} = \frac{\mu_{hnf}}{\rho_{hnf}}$$

1. Wall shear stress:

The dimensional wall shear stress along the stretching surface is

$$T_w = \mu_{hnf}\left(\frac{\partial u}{\partial r}\right)_{r=R}$$

Using the similarity transformation, the above expression reduces to

$$T_w = \mu_{hnf} U_0 \left(\frac{U_0}{\nu_{hnf} L}\right)^{1/2} f''(0)$$

where $f''(0)$ is the dimensionless wall velocity gradient.

2. Skin-friction Coefficient:

The local skin-friction coefficient is

$$C_f = \frac{T_w}{\rho_{hnf} U^2}$$

Introducing the local Reynolds number

$$Re_x = \frac{Ux}{\nu_{hnf}}$$

The dimensionless skin-friction coefficient becomes

$$C_f \, Re_x^{1/2} = f''(0)$$

3. Surface heat transfer rate (near the sheet):
The surface heat flux is defined by Fourier's law as

$$q_w = -k_{hnf} \left(\frac{\partial T}{\partial r} \right)_{r=R}$$

Using similarity variables, this reduces to

$$q_w = -k_{hnf}(T_w - T_\infty) \left(\frac{U_0}{\nu_{hnf} L} \right)^{1/2} \theta'(0)$$

where $\theta'(0)$ represents the dimensionless wall temperature gradient.

4. Local Nusselt Number:
The local Nusselt number is defined as

$$Nu_x = \frac{x q_w}{k_{hnf}(T_w - T_\infty)}$$

Substituting the similarity form of q_w, we obtain

$$Nu_x = -Re_x^{1/2} \, \theta'(0)$$

3. Discussions on the Results

In the present study, analytical and numerical investigations are performed to examine the steady magnetohydrodynamic (MHD) boundary-layer flow and heat transfer characteristics of a Al_2O_3 -MWCNT / engine-oil hybrid nanofluid on a cylindrical stretching surface embedded in a Darcy porous medium, in the presence of internal heat generation or absorption. The governing equations are transformed into a system of similarity equations and solved accordingly. The effects of various physical parameters, including the heat generation/absorption parameter and radiation absorption parameter, are systematically analyzed and validated through graphical illustrations and tabulated results. A set of standard dimensionless parameters is employed in the mathematical formulation. The graphical results are displayed in Figures 2–9, where subplots (a) and (b) represent the velocity and temperature profiles for the flat plate and stretching cylinder, respectively.

3.1. Parameter effects on velocity and temperature profiles

Figure 2*a* and 2*b* show how the temperature distribution $\theta(\eta)$ and its gradient are affected by the magnetic parameter M for a flat plate (Fig. 2*a*) and a stretching cylinder (Fig. 2*b*). The temperature profile inside the thermal boundary layer decreases for both geometries as M increases. This decrease is linked to the Lorentz force produced by the applied magnetic field, which inhibits thermal diffusion and opposes fluid motion, resulting in a thinner thermal boundary layer. Larger values of M accelerate the decay of $\theta(\eta)$ in the flat plate scenario (Fig. 2*a*) and increase the size of the temperature gradient close to the surface, suggesting a larger rate of surface heat transfer. The stretched cylinder (Fig. 2*b*) shows a similar pattern, although curvature effects make the magnetic parameter's impact more noticeable. It is evident from the inset graphs that raising M increases the temperature gradient at the wall, which raises the local Nusselt number. Overall, the stretching cylinder shows more sensitivity to magnetic effects than the flat plate, indicating the combined influence of magnetic forces and geometric curvature on heat transfer characteristics, even though the magnetic field suppresses the thermal boundary layer in both configurations.

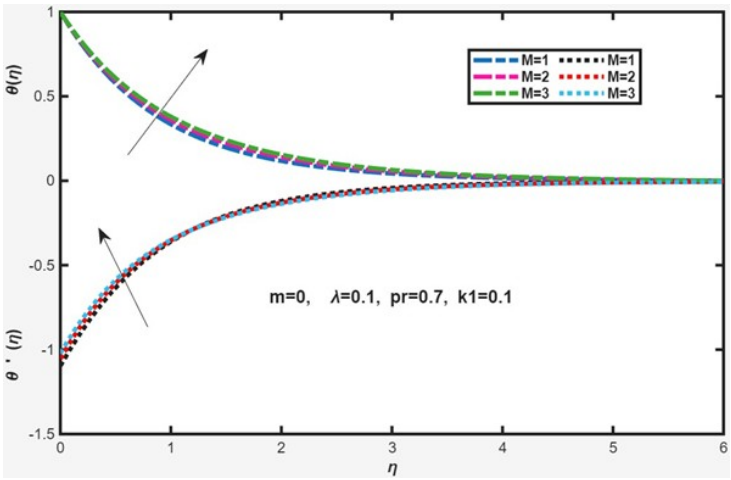

Figure 2a: For a flat plate, the temperature profile versus the magnetic parameter.

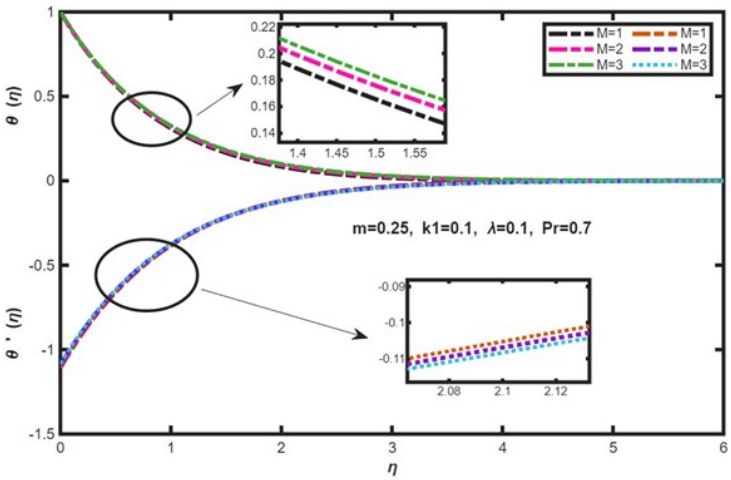

Figure 2b: Temperature profile versus magnetic parameter for a stretching cylinder.

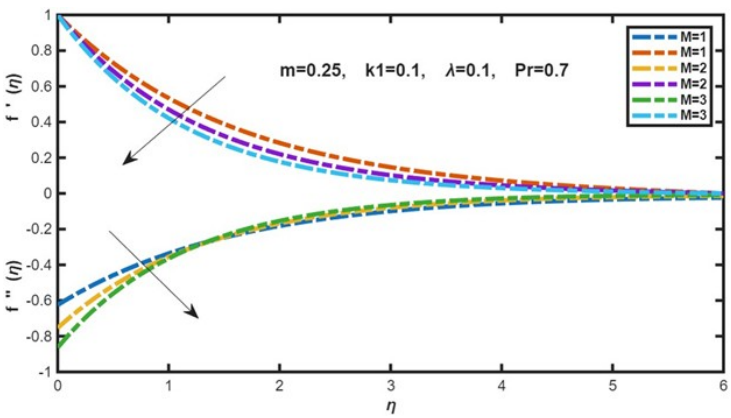

Figure 3a: Shear stress profile and velocity variation in relation to the magnetic parameter for a stretching cylinder.

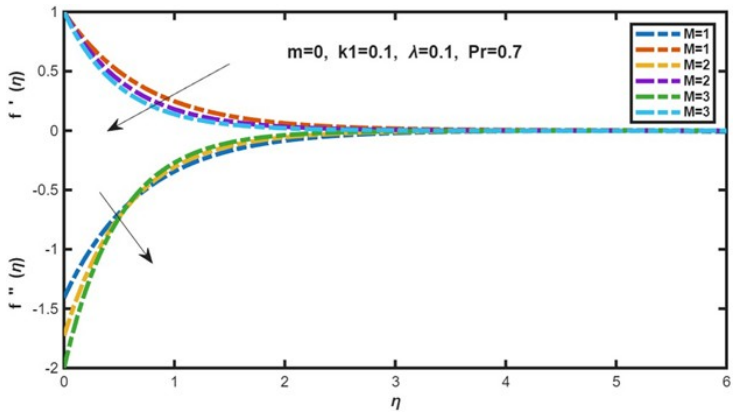

Figure 3b: Variation of velocity and shear stress profile versus magnetic parameter for a flat plate.

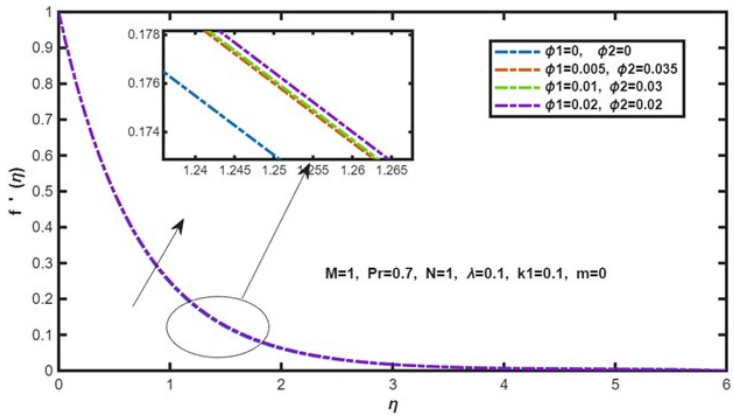

Figure 4a: Velocity profile versus volume fractions for a flat plate.

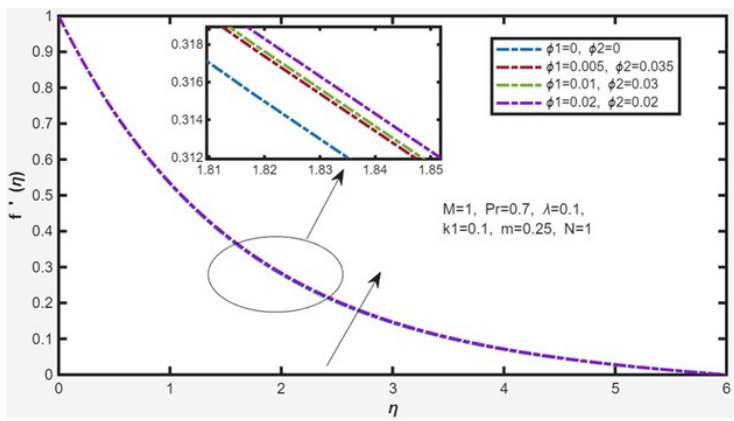

Figure 4b: Velocity profile versus volume fractions for a stretching cylinder.

The graphs show how the magnetic parameter M affects the velocity and shear stress profiles of an Al_2O_3–MWCNTs hybrid nanofluid using engine oil as the base fluid for a stretching cylinder in Fig.3*a* and a flat plate in Fig.3*b*. The Lorentz force produced by the applied magnetic field, which opposes fluid motion, causes the velocity to drop in both geometries as M increases. Because MWCNTs greatly

increase electrical conductivity, which results in increased momentum suppression and a narrower velocity boundary layer, this resistance is larger in the hybrid nanofluid. On the other hand, larger skin-friction coefficients are indicated by an increase in shear stress near the surface with increasing M. Because of the curvature-induced amplification of momentum diffusion, the stretching cylinder exhibits a stronger magnetic effect than the flat plate.

The impact of nanoparticle volume fractions on the velocity profile of an Al_2O_3–MWCNTs/engine oil hybrid nanofluid is shown in Fig.4*a* for a flat plate and in Fig.4*b* a stretching cylinder. When the volume fractions of Al2O3 and MWCNTs are increased, there is a noticeable drop in velocity across the boundary layer. This phenomenon is explained by the hybrid nanofluid's increased effective viscosity and density due to the presence of solid nanoparticles, which raises flow resistance. This effect is further enhanced by the presence of MWCNTs because of their strong interaction with the base fluid and high aspect ratio, which increases momentum diffusion. As a result, when the concentration of nanoparticles increases, the momentum boundary layer thickness decreases. The combined effect of surface curvature and hybrid nanoparticle loading is demonstrated by the stretching cylinder's somewhat greater velocity decrease in comparison to the flat plate. Near the surface, where velocity variations are more noticeable, the inset charts support these tendencies.

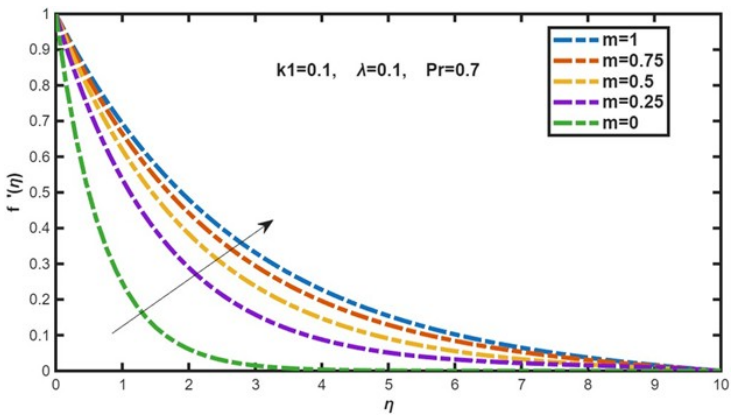

Figure 5a: Velocity profile versus curvature parameter.

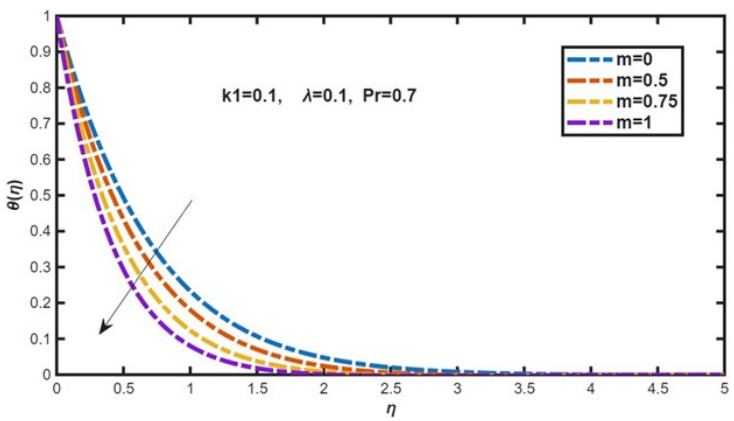

Figure 5b: Temperature profile versus curvature parameter.

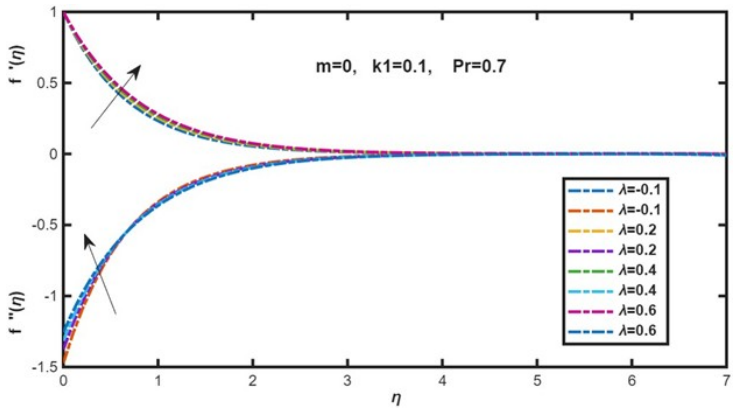

Figure 6a: For a flat plate, velocity and shear stress profile versus the mixed convection parameter.

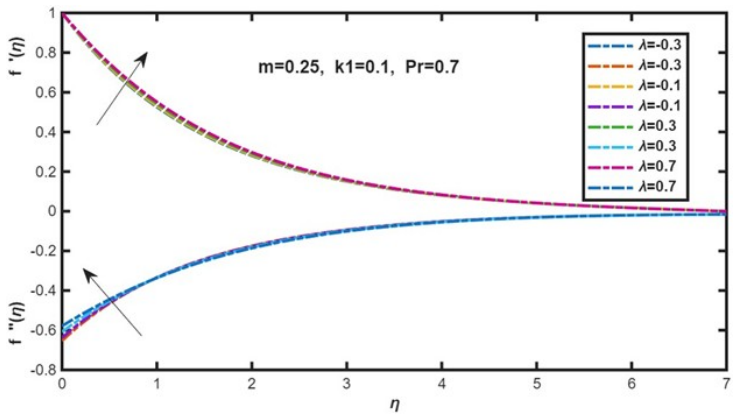

Figure 6b: For a stretching cylinder, velocity and shear stress profile versus the mixed convection parameter.

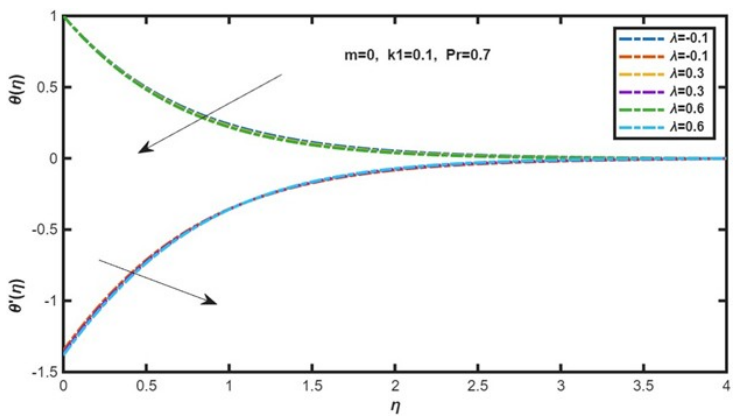

Figure 6c: For a flat plate, temperature and temperature gradient profile versus the mixed convection parameter.

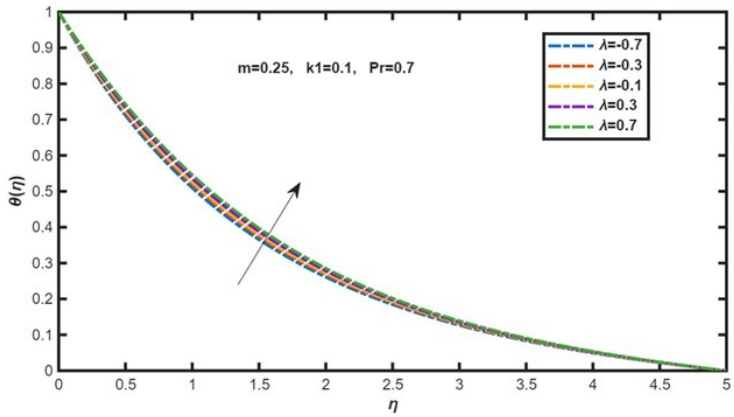

Figure 6d: For the stretching cylinder, the temperature profile versus the mixed convection parameter.

Fig.5*a* illustrates how the axial velocity for a stretched cylinder employing the Al_2O_3–MWCNT/engine-oil hybrid nanofluid under MHD circumstances varies with the curvature parameter. Since curvature encourages fluid stretching, larger curvature values result in a minor increase in near-wall velocity. The velocity steadily decreases further from the wall. In contrast to a pure fluid, the presence of hybrid nanoparticles enhances the engine oil's effective viscosity, suppressing flow motion and creating a larger momentum barrier layer. The Lorentz force acts as a resistive drag force as the magnetic field strength increases, further slowing down the electrically conducting hybrid nanofluid and flattening the velocity profile. Therefore, when compared to the non-magnetic condition, the combined impact of nanoparticle loading and MHD effects lowers the surface velocity gradient, indicating a decrease in skin-friction. Fig.5*b* shows how curvature affects the hybrid nanofluid boundary layer's temperature distribution. The hybrid nanofluid shows improved thermal transport capabilities, leading to higher temperature values and a thicker thermal boundary layer than traditional engine oil, because of the strong thermal conductivity of MWCNTs supported by Al_2O_3 particles. Surface stretching enhances convective transport and marginally lowers the temperature close to the wall as curvature rises. Nevertheless, the hybrid nanofluid's internal heat generation is increased when a heat source term is present, raising the temperature throughout the boundary layer and diminishing the wall temperature differential. On the other hand, a heat sink increases heat removal, which results in a thinner thermal layer, better surface heat transmission, and a faster temperature decrease. Because of its greater heat-conduction capability, the hybrid nanofluid reacts to the heat-source/sink effect more strongly than regular fluids.

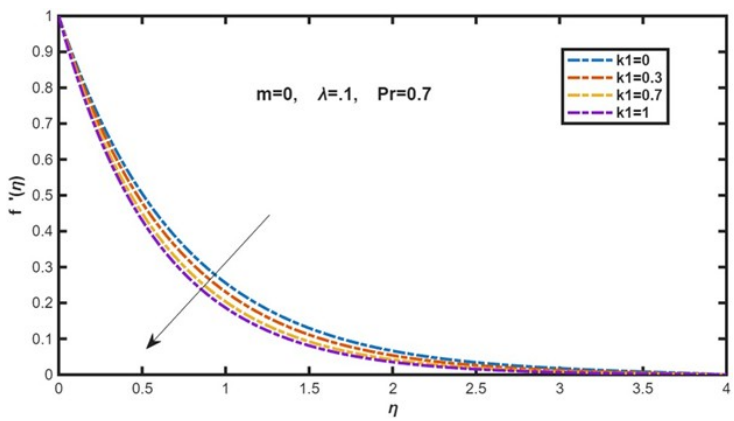

Figure 7a: For a flat plate, velocity profile versus permeability parameter.

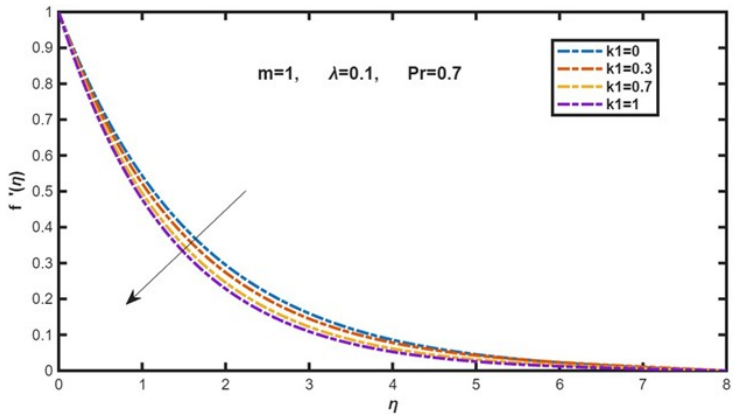

Figure 7b: For a stretching cylinder, velocity profile versus permeability parameter.

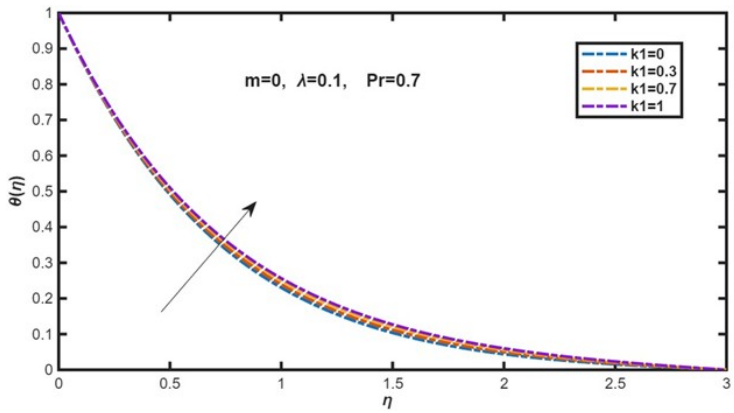

Figure 7c: For a flat plate, temperature profile versus permeability parameter.

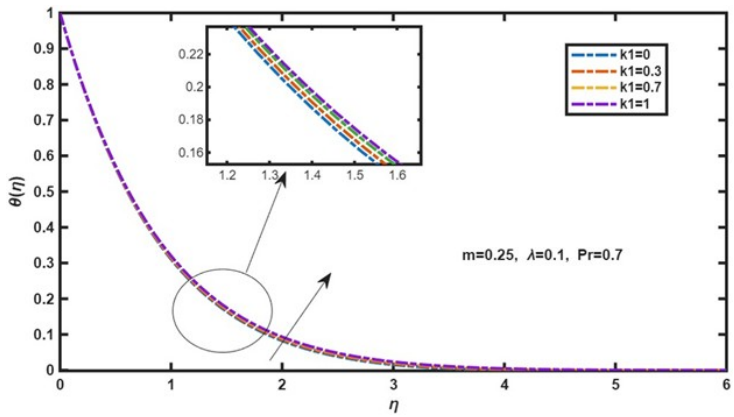

Figure 7d: For a stretching cylinder, temperature profile versus permeability parameter.

In Fig. 6*a* and Fig.6*b*, the velocity and shear-stress changes for buoyancy-aided and buoyancy-opposed flows in the hybrid nanofluid system are contrasted for a flat plate and a stretching cylinder. Thermal buoyancy energizes the flow and causes a slight acceleration of the boundary-layer motion in buoyancy-aided conditions ($\lambda > 0$), but the increase is reduced since the hybrid nanofluid has a higher viscosity

as a result of Al_2O_3–MWCNT particle loading. Momentum transport is slowed under MHD impact because the Lorentz force opposes buoyancy acceleration. Because of larger opposing pressures, shear stress increases in magnitude and velocity declines more quickly in buoyancy-opposed flow ($\lambda < 0$). In contrast to simple fluids, the hybrid-nanofluid viscosity and magnetic field work together to stabilize the boundary layer, resulting in thicker but smoother velocity profiles. Fig. 6*c* and Fig.6*d*, the impact of mixed convection and heat source/sink in the hybrid nanofluid is depicted. The temperature profile shifts upward in buoyancy-aided flow due to the increased thermal energy that encourages temperature rise within the boundary layer. This effect is amplified in the presence of a heat source. Because MWCNTs and Al_2O_3 particles provide high-conductivity thermal channels, the hybrid nanofluid effectively holds heat, resulting in a more noticeable temperature rise than in base oil. In heat-sink conditions, cooling takes over, the temperature drops dramatically, and the thermal boundary layer thins, increasing the rate of surface heat transfer. Because of its increased capacity to dissipate heat, the hybrid nanofluid exhibits better cooling performance in sink-dominated regimes.

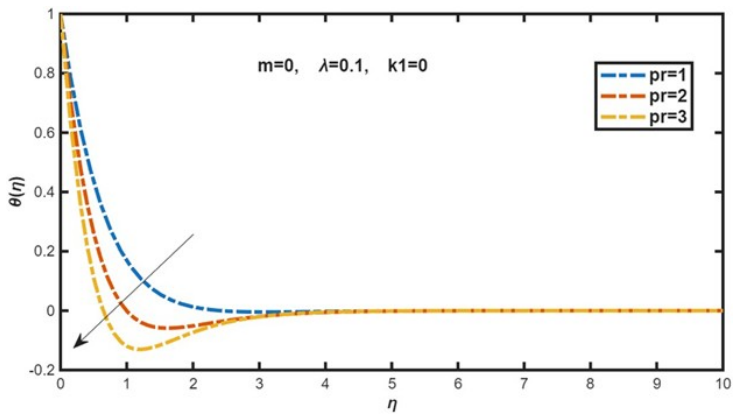

Figure 8a: For a flat plate, temperature profile versus Prandtl number.

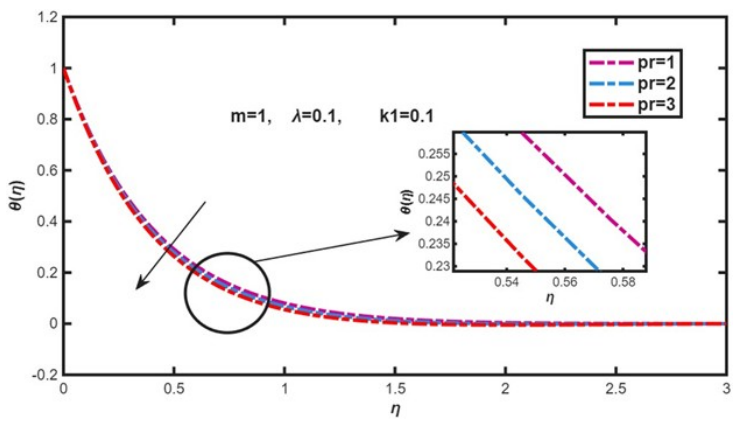

Figure 8b: For a stretching cylinder, temperature profile versus Prandtl number.

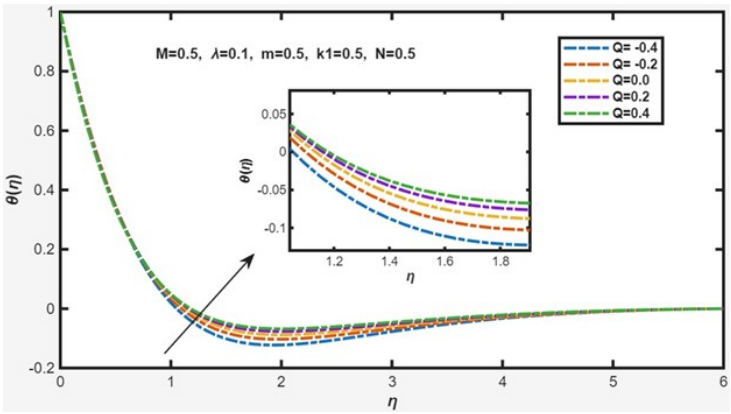

Figure 9: Temperature profile versus heat source parameter.

The impact of porous-medium permeability on the hybrid nanofluid flow is seen in Fig.7*a* to Fig.7*d*. Increasing permeability permits more fluid motion and less drag from the porous matrix, but the increase in velocity is still constrained in comparison to Newtonian fluids since the hybrid nanofluid has a higher effective viscosity than pure oil. Because the slower-moving hybrid nanofluid retains thermal energy more effectively, the temperature rises concurrently with permeability. The magnetic field and porous resistance work together to further reduce velocity and increase heat accumulation inside the porous layer when MHD processes are engaged. A heat sink counteracts this temperature increase by enhancing heat loss, while the presence of a heat source increases it.

Fig.8*a* and Fig.8*b* illustrate how engine-oil-based hybrid nanofluids, which usually have high Pr values, are affected by the Prandtl number. Thermal diffusivity falls as Pr rises, creating a thinner thermal boundary layer and a more pronounced temperature differential at the wall. The rate of heat transmission increases as a result. Because nanoparticle loading raises both viscosity and heat capacity, increasing the sensitivity of temperature transfer to Prandtl number, the hybrid nanofluid reacts significantly to changes in Pr. The heat-transfer enhancement increases in importance in a heat-sink condition. Fig.9 depicts the temperature profile along heat source parameter and found that heat production ($Q > 0$) raises the hybrid nanofluid's internal energy, resulting in a thicker thermal layer and a higher temperature. Whereas heat absorption ($Q < 0$) lowers temperature by removing energy from the fluid. The hybrid nanofluid is appropriate for thermal energy regulation in high-temperature engineering applications because it facilitates improved micro-convection and thermal conduction and reacts more effectively to changes in the heat source.

Table 1: Thermophysical characteristics of base fluid and hybrid nanoparticles by Tulu and Ibrahim [41]

Physical properties	**Base fluid**	**Hybrid nanoparticles**	
	Engine oil (EO)	**MWCNTs**	**Al_2O_3**
$\rho\,(\mathrm{kg/m^3})$	884	1600	3970
$C_p\,(\mathrm{J/kg\,K})$	1910	796	765
$k\,(\mathrm{W/m\,K})$	0.144	3000	40
$\beta\,(10^{-5}\,\mathrm{K^{-1}})$	70	44	0.85

Table 2: Nabel et al. [42] provide the thermophysical characteristics of hybrid nanofluids

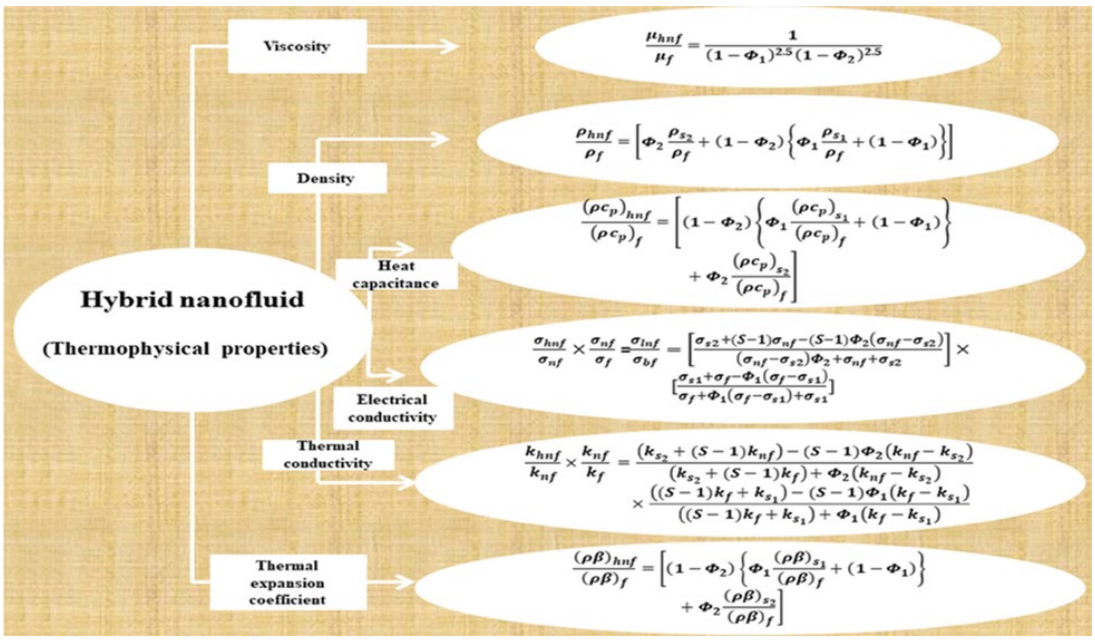

Table 3: Calculation of Nusselt Number $-\theta'(0)$ (N-temperature exponent and Pr – Prandtl number)

N\Pr	0.1	0.72	1.0	3.0	10.0	100.0
-3	0.365073	0.364789	0.364662	0.363783	0.361040	0.348120
-2	0.365089	0.364903	0.364819	0.364245	0.362459	0.354219
-1	0.365105	0.365017	0.364977	0.364705	0.363860	0.360216
0	0.365121	0.365130	0.365135	0.365163	0.365249	0.365728
1	0.365137	0.365244	0.365292	0.365621	0.366624	0.371911
2	0.365153	0.365358	0.365449	0.366076	0.367983	0.377612
3	0.365169	0.365471	0.365606	0.366530	0.369330	0.383216

In Table 3 presents the local Nusselt number numerically for different values of the temperature exponent N and Prandtl number Pr. For a constant Pr, the Nusselt number is observed to gradually increase with increasing N, indicating better surface heat transfer for greater wall temperature differences. Conversely, at a given N, an increase in the Prandtl number results in a noticeable rise, demonstrating the shrinkage of the thermal boundary layer associated with higher Pr fluids. Overall, the table indicates that both the temperature exponent and the Prandtl number have a substantial impact on the heat transfer rate at the cylinder surface.

4. Conclusion

In this study, a comprehensive analysis has been conducted for engine-oil-based Al_2O_3–MWCNT hybrid nanofluid flow past a stretching cylinder embedded in a porous medium in the presence of a heat source/sink effect. A detailed MHD mixed convection model has been formulated and numerically solved using the BVP4C technique. The effects of key physical parameters, including the magnetic field strength and heat generation/absorption parameter, on the flow and thermal characteristics have been systematically examined through graphical illustrations. The results reveal that momentum transport decreases with increasing magnetic field intensity and heat generation, whereas the inclusion of hybrid nanoparticles significantly enhances the thermal performance of the fluid. The developed model demonstrates potential applicability in energy engineering systems, advanced thermal management processes, and lubrication technologies.

- A comprehensive hybrid-nanofluid extension of the stretching-cylinder MHD problem has been developed and solved.
- Due to their enhanced thermal conductivity synergy, hybrid nanoparticles significantly enhance heat transfer.
- Boundary-layer transport behavior is significantly influenced by magnetic, porosity, and heat-source parameters.
- The developed model can serve as a computational platform for advanced fluid engineering and energy system cooling applications

5. Validation

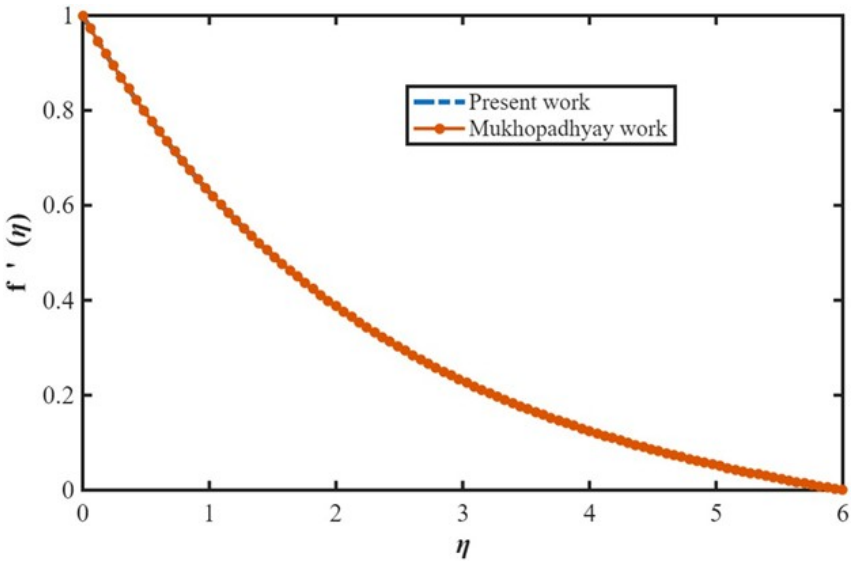

Figure 10a: Comparison of velocity profile

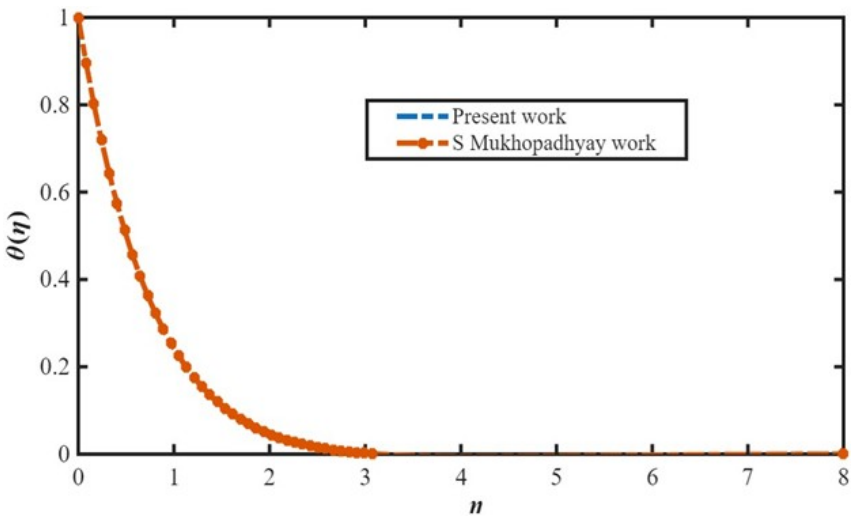

Figure 10b: Comparison of temperature profile

The main objective of this research is to determine the temperature and velocity distributions of hybrid nanofluids flowing through a porous medium in the presence of a heat source/sink and a magnetic field. Additionally, the study aims to compare these profiles with those obtained by S. Mukhopadhyay [1], who conducted a similar investigation in the absence of a magnetic field and heat source/sink. Furthermore, when $Q = 0$, $\phi_1 = \phi_2 = 0$, $\alpha = 0$, and $M = 0$, the obtained velocity and temperature profiles coincide with the results reported by Reddy et al. [43] and Ismail et al. [17].

6. Nomenclature

C_f	Skin friction coefficient	Pr	Prandtl number
C_p	Specific heat capacity (J/kg·K)	Q	Heat source/sink parameter
f	Dimensionless stream function	q_w	Heat transfer from the cylinder surface
g	Gravitational force	R	Radius of cylinder
k	Thermal conductivity (W/m·K)	r	Radial coordinate (m)
K	Permeability of porous medium (m^2)	Re_x	Local Reynolds number
M	Magnetic parameter	T	Temperature of nanofluid
m	Curvature parameter	T_w	Surface temperature
N	Temperature exponent	T_∞	Ambient temperature
Nu_x	Local Nusselt number	u, v	Velocity components (m/s)
x	Axial coordinate (m)		

6.1. Greek symbols

α	Thermal diffusivity	λ	Mixed convection parameter
η	Similarity variable	β	Thermal expansion coefficient
θ	Similarity temperature function	ψ	Stream function
ρ	Fluid density (kg/m^3)	σ	Electrical conductivity
ϕ_1, ϕ_2	Nanoparticle volume fractions	μ	Dynamic viscosity
ν	Kinematic viscosity		

6.2. Subscripts

f	Fluid
nf	Nanofluid
hnf	Hybrid nanofluid
w	Surface condition
∞	Far field

Acknowledgments

The authors thank the management of REVA University for their support in carrying out this research work.

References

1. Mukhopadhyay, S., *Mixed convection boundary layer flow along a stretching cylinder in porous medium.* Journal of Petroleum Science and Engineering 96, 73–78 (2012).
2. Chandrasekar, M., Suresh, S., and Senthilkumar, T., *Mechanisms proposed through experimental investigations on thermophysical properties and forced convective heat transfer characteristics of various nanofluids–A review.* Renewable and Sustainable Energy Reviews 16(6), 3917–3938 (2012).
3. Devi, S. A., and Devi, S. S. U., *Numerical investigation of hydromagnetic hybrid Cu–Al_2O_3/water nanofluid flow over a permeable stretching sheet with suction.* International Journal of Nonlinear Sciences and Numerical Simulation 17(5), 249–257 (2016).
4. Ishak, A., Nazar, R., and Pop, I., *Uniform suction/blowing effect on flow and heat transfer due to a stretching cylinder.* Applied Mathematical Modelling 32(10), 2059–2066 (2008).
5. Wang, C. Y., *Fluid flow due to a stretching cylinder.* Physics of Fluids 31(3), 466 (1988).
6. Kumari, M., and Nath, G., *Mixed convection boundary layer flow over a thin vertical cylinder with localized injection/suction and cooling/heating.* International Journal of Heat and Mass Transfer 47(5), 969–976 (2004).

7. Elbarbary, E. M. E., and Elgazery, N. S., *Flow and heat transfer of a micropolar fluid in an axisymmetric stagnation flow on a cylinder with variable properties and suction (numerical study)*. Acta Mechanica 176(3), 213–229 (2005).

8. Datta, P., Anilkumar, D., Roy, S., and Mahanti, N. C., *Effect of non-uniform slot injection (suction) on a forced flow over a slender cylinder*. International Journal of Heat and Mass Transfer 49(13–14), 2366–2371 (2006).

9. Sundar, L. S., Sharma, K. V., Singh, M. K., and Sousa, A. C. M., *Hybrid nanofluids preparation, thermal properties, heat transfer and friction factor–a review*. Renewable and Sustainable Energy Reviews 68, 185–198 (2017).

10. Hemmat Esfe, M., Saedodin, S., Mahian, O., and Wongwises, S., *Thermal conductivity of Al_2O_3/water nanofluids: measurement, correlation, sensitivity analysis, and comparisons with literature reports*. Journal of Thermal Analysis and Calorimetry 117(2), 675–681 (2014).

11. Sarkar, J., Ghosh, P., and Adil, A., *A review on hybrid nanofluids: recent research, development and applications*. Renewable and Sustainable Energy Reviews 43, 164–177 (2015).

12. Saeed, A., Alghamdi, W., Mukhtar, S., Shah, S. I. A., Kumam, P., Gul, T., and Kumam, W., *Darcy–Forchheimer hybrid nanofluid flow over a stretching curved surface with heat and mass transfer*. PLoS One 16(5), e0249434 (2021).

13. Manjunatha, S., Kuttan, B. A., Jayanthi, S., Chamkha, A., and Gireesha, B. J., *Heat transfer enhancement in the boundary layer flow of hybrid nanofluids due to variable viscosity and natural convection*. Heliyon 5(4) (2019).

14. Nadeem, S., and Lee, C., *Boundary layer flow of nanofluid over an exponentially stretching surface*. Nanoscale Research Letters 7(1), 94 (2012).

15. Chamkha, A. J., *Hydromagnetic three-dimensional free convection on a vertical stretching surface with heat generation or absorption*. International Journal of Heat and Fluid Flow 20(1), 84–92 (1999).

16. Nath, R. S., and Deka, R. K., *A numerical investigation of the MHD ternary hybrid nanofluid (Cu–Al_2O_3–TiO_2/H_2O) past a vertically stretching cylinder in a porous medium with thermal stratification*. Journal of Advanced Research in Fluid Mechanics and Thermal Sciences 116(1), 78–96 (2024).

17. Ismail, M., and Gururaj, D. M., *Numerical investigation on nonlinear radiative magneto hydrodynamics hybrid nanofluid flow past a stretching cylinder embedded in porous medium*. Journal of Nanofluids 12(3), 809–818 (2023).

18. Hayat, T., Qayyum, S., Alsaedi, A., and Shafiq, A., *Inclined magnetic field and heat source/sink aspects in flow of nanofluid with nonlinear thermal radiation*. International Journal of Heat and Mass Transfer 103, 99–107 (2016).

19. Ali, M., Alim, M. A., and Alam, M. S., *Heat transfer boundary layer flow past an inclined stretching sheet in the presence of magnetic field*. International Journal of Advanced Research in Technology 3(5), 34–40 (2014).

20. Ismail, M., and Gururaj, D. M., *Numerical investigation on nonlinear radiative magneto hydrodynamics hybrid nanofluid flow past a stretching cylinder embedded in porous medium*. Journal of Nanofluids 12(3), 809–818 (2023).

21. Gururaj, A. D. M., and Devi, S. A., *MHD boundary layer flow with heat transfer, variable conductivity and nonlinear Rosseland approximation thermal radiation effects past a nonlinearly stretching porous surface with a power-law velocity*. International Journal of Applied Engineering Research 10, 8073–8090 (2015).

22. Krishna, M. V., and Chamkha, A. J., *Hall effects on MHD squeezing flow of a water-based nanofluid between two parallel disks*. Journal of Porous Media 22(2) (2019).

23. Krishna, M. V., and Chamkha, A. J., *Hall and ion slip effects on MHD rotating boundary layer flow of nanofluid past an infinite vertical plate embedded in a porous medium*. Results in Physics 15, 102652 (2019).

24. Krishna, M. V., Ahamad, N. A., and Chamkha, A. J., *Radiation absorption on MHD convective flow of nanofluids through vertically travelling absorbent plate*. Ain Shams Engineering Journal 12(3), 3043–3056 (2021).

25. Krishna, M. V., Ahamad, N. A., and Aljohani, A. F., *Thermal radiation, chemical reaction, Hall and ion slip effects on MHD oscillatory rotating flow of micro-polar liquid*. Alexandria Engineering Journal 60(3), 3467–3484 (2021).

26. Krishna, M. V., and Chamkha, A. J., *Hall and ion slip effects on MHD rotating flow of elastico-viscous fluid through porous medium*. International Communications in Heat and Mass Transfer 113, 104494 (2020).

27. Khan, M., Malik, R., and Hussain, M., *Nonlinear radiative heat transfer to stagnation-point flow of Sisko fluid past a stretching cylinder*. AIP Advances 6(5) (2016).

28. Hayat, T., Tamoor, M., Khan, M. I., and Alsaedi, A., *Numerical simulation for nonlinear radiative flow by convective cylinder*. Results in Physics 6, 1031–1035 (2016).

29. Hayat, T., Rashid, M., Alsaedi, A., and Asghar, S., *Nonlinear convective flow of Maxwell nanofluid past a stretching cylinder with thermal radiation and chemical reaction*. Journal of the Brazilian Society of Mechanical Sciences and Engineering 41(2), 86 (2019).

30. Choi, S. U. S., and Eastman, J. A., *Enhancing thermal conductivity of fluids with nanoparticles*. Journal of Applied Mechanics 1, 1 (1995).

31. Hussein, A. M., Noor, M. M., Kadirgama, K., Ramasamy, D., and Rahman, M. M., *Heat transfer enhancement using hybrid nanoparticles in ethylene glycol through a horizontal heated tube*. International Journal of Automotive and Mechanical Engineering 14(2), 4183–4195 (2017).

32. Hamid, K. A., Azmi, W. H., Nabil, M. F., and Mamat, R., *Improved thermal conductivity of TiO_2–SiO_2 hybrid nanofluid in ethylene glycol and water mixture*. IOP Conference Series: Materials Science and Engineering 257(1), 012067 (2017).

33. Boukerma, K., and Kadja, M., *Convective heat transfer of Al_2O_3 and CuO nanofluids using various mixtures of water–ethylene glycol as base fluids*. Engineering, Technology & Applied Science Research 7(2), 1496–1503 (2017).

34. Wang, C. Y., *Fluid flow due to a stretching cylinder*. Physics of Fluids 31(3), 466 (1988).

35. Maskeen, M. M., Zeeshan, A., Mehmood, O. U., and Hassan, M., *Heat transfer enhancement in hydromagnetic alumina–copper/water hybrid nanofluid flow over a stretching cylinder*. Journal of Thermal Analysis and Calorimetry 138(2), 1127–1136 (2019).

36. Poply, V., *Heat transfer in a MHD nanofluid over a stretching sheet*. In: Heat Transfer–Design, Experimentation and Applications. IntechOpen (2020).

37. Ismail, M., and Gururaj, A. D. M., *Radiative MHD flow of hybrid nanofluid past a porous stretching cylinder for heat transfer enhancement*. Heat Transfer 50(4), 4019–4038 (2021).

38. Alagumalai, A., Qin, C., Solomin, E., Yang, L., Zhang, P., Otanicar, T., and Mahian, O., *Conceptual analysis framework development to understand barriers of nanofluid commercialization*. Nano Energy 92, 106736 (2022).

39. Dogonchi, A. S., Waqas, M., Afshar, S. R., Seyyedi, S. M., Hashemi-Tilehnoee, M., Chamkha, A. J., and Ganji, D. D., *Investigation of magneto-hydrodynamic fluid squeezed between two parallel disks by considering Joule heating, thermal radiation, and adding different nanoparticles*. International Journal of Numerical Methods for Heat & Fluid Flow 30(2), 659–680 (2020).

40. Dogonchi, A. S., Mishra, S. R., Chamkha, A. J., Ghodrat, M., Elmasry, Y., and Alhumade, H., *Thermal and entropy analyses on buoyancy-driven flow of nanofluid inside a porous enclosure with two square cylinders: Finite element method*. Case Studies in Thermal Engineering 27, 101298 (2021).

41. Tulu, A., and Ibrahim, W., *Mixed convection hybrid nanofluids flow of MWCNTs–Al_2O_3/engine oil over a spinning cone with variable viscosity and thermal conductivity*. Heat Transfer 50(4), 3776–3799 (2021).

42. Nabil, M. F., Azmi, W. H., Hamid, K. A., Zawawi, N. N. M., Priyandoko, G., and Mamat, R., *Thermo-physical properties of hybrid nanofluids and hybrid nanolubricants: a comprehensive review on performance*. International Communications in Heat and Mass Transfer 83, 30–39 (2017).

43. Reddy, Y. D., Goud, B. S., Nisar, K. S., Alshahrani, B., Mahmoud, M., and Park, C., *Heat absorption/generation effect on MHD heat transfer fluid flow along a stretching cylinder with a porous medium*. Alexandria Engineering Journal 64, 659–666 (2023).

Poornima Samaje,
https://orcid.org/0009-0006-0743-3118
Research Scholar,
Department of Mathematics,
School of Applied Sciences,
REVA University,
Bengaluru 560064,
Karnataka, India.
LE Society's S.Nijalingappa College,
Rajajinagar, Bengaluru-560010, Karnataka, India.
E-mail address: R21PMT16@reva.edu.in

and

Salma Allabaksh,
https://orcid.org/0000-0003-1003-9315
Department of Mathematics,
School of Applied Sciences,
REVA University
Bengaluru 560064
Karnataka,
India.
E-mail address: salma.alla@gmail.com

and

Sibyala Vijayakumar Varma,
https://orcid.org/0000-0002-9757-9316
Department of Mathematics,
School of Applied Sciences,
REVA University
Bengaluru 560064
Karnataka,
India.
E-mail address: svijayakumarvarma@yahoo.co.in

and

Hanumagowda Bannihalli Naganagowda,
https://orcid.org/0000-0002-1210-0231
Department of Mathematics,
School of Applied Sciences,
REVA University
Bengaluru 560064
Karnataka,
India.
E-mail address: hanumagowda123@rediffmail.com